Research Square

Preprints are preliminary reports that have not undergone peer review.
They should not be considered conclusive, used to inform clinical practice,
or referenced by the media as validated information.

Dynamics and synchronization of the complex simplified Lorenz system

Mengxin Jin (mengxin_jin@csu.edu.cn)
Central South University https://orcid.org/0000-0002-8703-3889
Kehui Sun
Central South University
Huihai Wang
Central South University

Research Article

Keywords: Complex chaos, Simplified Lorenz system, Coexisting attractors, Extreme multistability, Adaptive control, Generalized function projective synchronization

Posted Date: April 28th, 2021

DOI: https://doi.org/10.21203/rs.3.rs-412035/v1

License: This work is licensed under a Creative Commons Attribution 4.0 International License.
Read Full License

Version of Record: A version of this preprint was published at Nonlinear Dynamics on September 18th, 2021. See the published version at https://doi.org/10.1007/s11071-021-06905-2.

Nonlinear Dynamics manuscript No.
(will be inserted by the editor)

Dynamics and synchronization of the complex simplified Lorenz system

Mengxin Jin · Kehui Sun · Huihai Wang

Received: date / Accepted: date

Abstract In this paper, the complex simplified Lorenz system is proposed. It is the complex extension of the simplified Lorenz system. Dynamics of the proposed system are investigated by theoretical analysis as well as numerical simulation, including bifurcation diagram, Lyapunov exponent spectrum, phase portraits, Poincaré section, and basins of attraction. The results show that the complex simplified Lorenz system has non-trivial circular equilibria and displays abundant and complicated dynamical behaviors. Particularly, the coexistence of infinitely many attractors, i.e., extreme multistability, is discovered in the proposed system. Furthermore, the adaptive complex generalized function projective synchronization between two complex simplified Lorenz systems with unknown parameter is achieved. Based on Lyapunov stability theory, the corresponding adaptive controllers and parameter update law are designed. The numerical simulation results demonstrate the effectiveness and feasibility of the proposed synchronization scheme. It provides a theoretical and experimental basis for the applications of the complex simplified Lorenz system.

Keywords Complex chaos · Simplified Lorenz system · Coexisting attractors · Extreme multistability · Adaptive control · Generalized function projective synchronization

1 Introduction

Since Lorenz discovered the first chaotic attractor in 1963 [1], chaos has been extensively investigated over the last few decades due to its great importance and broad applications. Particularly, in 1982, Fowler et al. [2] derived the complex chaotic Lorenz equations, which opened the prelude to the study of complex chaos. However, compared with the limited studies of chaos in complex domain, there are a large quantity of articles of chaos in real domain. As a matter of fact, in the real world, many physical phenomena can be described by complex-variable nonlinear dynamical equations, such as thermal convection of liquid flows, detuned lasers and complex nonlinear oscillators [3–7]. The complex chaotic system, i.e., the chaotic system with complex variables, is a kind of typical complex dynamical system, which is obtained by extending the chaotic system from real domain to complex domain. Due to the existence of complex variables, dynamical behaviors of the complex chaotic system tend to be more abundant and complicated, which indicates the wide scope of applications, especially for secure communication and digital encryption [8–12].

Apart from the above-mentioned complex Lorenz system, some other complex chaotic systems have been proposed and investigated theoretically and numerically, such as the complex Chen system [13], complex Lü system [13], hyperchaotic complex Lorenz system [14] and hyperchaotic complex Lü system [15]. On the other hand, it is well known that the synchronization of chaotic systems plays an important role in chaotic secure communication. Therefore, some scholars also focused their attention on the study of chaos control and synchronization of complex chaotic systems in recent years, and a great number of synchronization schemes have been proposed, such as complete synchronization [16], lag synchronization [17], complex modified projective synchronization [18], adaptive impulsive synchronization [19], adaptive complex modified projective synchroniza-

M. Jin · K. Sun (✉) · H. Wang
School of Physics and Electronics, Central South University, Changsha 410083, China
E-mail: kehui@csu.edu.cn

tion [20], combination complex synchronization [21], adaptive complex modified hybrid function projective synchronization [22], and adaptive complex modified function projective synchronization [23]. However, the investigation of generalized synchronization of complex chaotic systems, where the complex drive and response systems synchronize with respect to a given functional relationship, was rarely reported. Only in [24], Wang et al. discussed the adaptive complex generalized synchronization of a memristor-based hyperchaotic complex Lü system. Furthermore, to better enhance the anti-attack and anti-translated performance of the transmitted signals in chaotic secure communication, it is significant and meaningful to investigate the complex generalized function projective synchronization of complex chaotic systems. To the best of our knowledge, although the generalized function projective synchronization of real-variable chaotic systems has been studied [25,26], the complex generalized function projective synchronization of complex chaotic systems was seldom discussed.

Recently, the coexistence of infinitely many attractors in chaotic systems, which is defined as extreme multistability, has become another research hotspot. In fact, the extreme multistability is an intrinsic property of many nonlinear dynamical systems. It means the coexistence of infinitely many asymptotic stable states for a given set of parameters. The state mainly depends on initial conditions. At present, the phenomenon of extreme multistability is found in some nonlinear circuits and dynamical systems [27–31]. Particularly, Bao et al. [32] discovered the hidden extreme multistability in a memristive hyperchaotic system. Lai et al. [33] established a simple three-dimensional chaotic system with infinitely many coexisting attractors based on the Sprott B system [34]. Furthermore, Li et al. [35] successfully doubled the number of the coexisting attractors by applying the offset boosting technique in combination with the absolute-value function. Generally, the chaotic system with multiple coexisting attractors is considered to be more complicated than the chaotic system with single attractor, and thus has more potential values in practical applications [36]. However, the coexistence of infinitely many attractors in complex chaotic systems has not been effectively explored so far.

Motivated by the above discussion, in this paper, by extending the real state variables from real domain to complex domain, the complex simplified Lorenz system is proposed. It is the complex extension of the simplified Lorenz system [37]. Dynamics and synchronization of the proposed system are investigated theoretically and numerically. The results show that the complex simplified Lorenz system has non-trivial circular equilibria, and exhibits abundant and complicated dynamical behaviors. Particularly, the coexistence of infinitely many attractors, i.e., extreme multistability, is found in this system. Furthermore, the adaptive complex generalized function projective synchronization between two complex simplified Lorenz systems with unknown parameter is achieved. Based on Lyapunov stability theory, the adaptive controllers and parameter update law are designed. The numerical simulation results demonstrate the effectiveness and feasibility of the proposed synchronization scheme.

The rest of this paper is organized as follows. In Sec. 2, the complex simplified Lorenz system is proposed, and basic dynamics of the proposed system is investigated theoretically and numerically. In Sec. 3, the adaptive complex generalized function projective synchronization between two complex simplified Lorenz systems with unknown parameter is discussed. The numerical simulation results are presented to verify the effectiveness and feasibility of the proposed synchronization scheme. Finally, the main conclusions are summarized in Sec. 4.

2 The complex simplified Lorenz system and its basic dynamics

In 2009, Sun and Sprott [37] simplified the classic Lorenz system, and proposed the simplified Lorenz system with only one bifurcation parameter. This system has similar dynamical properties to the Lorenz system, but its algebraic form is simpler. It is suitable for the study of chaos control, synchronization and circuit implementation, where serving as a simple model of chaos in real domain. The simplified Lorenz system is described by

$$\begin{cases} \dot{x}_1 = 10(x_2 - x_1), \\ \dot{x}_2 = (24 - 4c)x_1 + cx_2 - x_1x_3, \\ \dot{x}_3 = -8x_3/3 + x_1x_3, \end{cases} \tag{1}$$

where $x_1, x_2, x_3 \in \mathbb{R}$ are real state variables, and $c \in \mathbb{R}$ is the bifurcation parameter of system (1). Here, we extend the real state variables x_1, x_2 from real domain to complex domain, and obtain the complex simplified Lorenz system, which is written in the following form

$$\begin{cases} \dot{x}_1 = 10(x_2 - x_1), \\ \dot{x}_2 = (24 - 4c)x_1 + cx_2 - x_1x_3, \\ \dot{x}_3 = -8x_3/3 + 1/2(\bar{x}_1x_2 + x_1\bar{x}_2), \end{cases} \tag{2}$$

where $x_1, x_2 \in \mathbb{C}$ are complex state variables, $x_3 \in \mathbb{R}$ is a real state variable, and $c \in \mathbb{R}$ is the bifurcation parameter of system (2). In addition, $\bar{x}_1, \bar{x}_2$ stands for the complex conjugate variables of x_1, x_2, respectively.

For the convenience of dynamics analysis, setting $x_1 = u_1 + ju_2$, $x_2 = u_3 + ju_4$, $x_3 = u_5$, where $j = \sqrt{-1}$, and equating the real and imaginary parts of system (2), we obtain

$$\begin{cases} \dot{u}_1 = 10(u_3 - u_1), \\ \dot{u}_2 = 10(u_4 - u_2), \\ \dot{u}_3 = (24 - 4c)u_1 + cu_3 - u_1u_5, \\ \dot{u}_4 = (24 - 4c)u_2 + cu_4 - u_2u_5, \\ \dot{u}_5 = -8u_5/3 + u_1u_3 + u_2u_4, \end{cases} \tag{3}$$

where $u_1, u_2, u_3, u_4, u_5 \in \mathbb{R}$ are real state variables, and $c \in \mathbb{R}$ is the bifurcation parameter of system (3).

2.1 Symmetry and invariance

System (3) is symmetric and invariant under the coordinates transformation: $(u_1, u_2, u_3, u_4, u_5) \to (-u_1, -u_2, -u_3, -u_4, u_5)$, i.e., reflection about u_5-axis. In addition, this symmetry and invariance are accurate for all values of the parameter c.

2.2 Dissipation and the existence of attractors

The rate of volume contraction of system (3) is given by the Lie derivative

$$\frac{1}{V}\frac{\mathrm{d}V}{\mathrm{d}t} = \sum_{k=1}^{5}\frac{\mathrm{d}\dot{u}_k}{\mathrm{d}t} = 2c - \frac{68}{3} = p, \tag{4}$$

which can be solved to yield

$$V(t) = V(0)e^{pt}. \tag{5}$$

If $p < 0$, i.e., $c < 34/3$, then system (3) is dissipative. It means all the trajectories of system (3) contract at an exponential rate p onto an attractor of zero volume that can be a fixed point, a limit cycle or a strange attractor when $t \to +\infty$.

2.3 Equilibria and their stability

To get the equilibria of system (3), we set the right part of system (3) to zero, and obtain the following nonlinear equations

$$\begin{cases} 10(u_3 - u_1) = 0, \\ 10(u_4 - u_2) = 0, \\ (24 - 4c)u_1 + cu_3 - u_1u_5 = 0, \\ (24 - 4c)u_2 + cu_4 - u_2u_5 = 0, \\ -8u_5/3 + u_1u_3 + u_2u_4 = 0. \end{cases} \tag{6}$$

Obviously, the origin $E_0 = (0, 0, 0, 0, 0)$ is one of the solutions of Eq. (6), and it's easy to get the non-trivial solutions of Eq. (6), which can be written as

$$u_1 = u_3 = r\cos\theta, u_2 = u_4 = r\sin\theta, u_5 = \frac{3}{8}r^2, \tag{7}$$

where $r = \sqrt{64 - 8c}$, and $\theta \in [0, 2\pi]$. Therefore, system (3) has non-trivial circular equilibria $E_\theta = (r\cos\theta, r\sin\theta, r\cos\theta, r\sin\theta, 3r^2/8)$.

To study the stability of E_0, we calculate the Jacobian matrix of system (3) at E_0 as

$$\boldsymbol{J}_0 = \begin{bmatrix} -10 & 0 & 10 & 0 & 0 \\ 0 & -10 & 0 & 10 & 0 \\ 24 - 4c & 0 & c & 0 & 0 \\ 0 & 24 - 4c & 0 & c & 0 \\ 0 & 0 & 0 & 0 & -8/3 \end{bmatrix}, \tag{8}$$

and its eigenvalues satisfy the following characteristic equation

$$\left(\mu + \frac{8}{3}\right)\left[\mu^2 + (10 - c)\mu + 30c - 240\right]^2 = 0, \tag{9}$$

thus we have $\mu_1 = -8/3$, and the other four eigenvalues satisfy the following equation

$$\left[\mu^2 + (10 - c)\mu + 30c - 240\right]^2 = 0. \tag{10}$$

According to Routh-Hurwitz criterion, if $10 - c > 0$ and $30c - 240 > 0$, i.e., $c \in (8, 10)$, then E_0 is stable, otherwise it's unstable. In addition, to study the stability of E_θ, we calculate the Jacobian matrix of system (3) at E_θ as

$$\boldsymbol{J}_\theta = \begin{bmatrix} -10 & 0 & 10 & 0 & 0 \\ 0 & -10 & 0 & 10 & 0 \\ -c & 0 & c & 0 & -r\cos\theta \\ 0 & -c & 0 & c & -r\sin\theta \\ r\cos\theta & r\sin\theta & r\cos\theta & r\sin\theta & -8/3 \end{bmatrix}, \tag{11}$$

and their eigenvalues satisfy the same characteristic equation, which is written as

$$\begin{aligned} \mu(\mu + 10 - c)\Bigg[\mu^3 + \left(\frac{38}{3} - c\right)\mu^2 \\ + \left(r^2 + \frac{80}{3} - \frac{8}{3}c\right)\mu + 20r^2\Bigg] = 0, \end{aligned} \tag{12}$$

thus we have $\mu_1 = 0$, $\mu_2 = c - 10$, and the other three eigenvalues satisfy the following equation

$$\mu^3 + \left(\frac{38}{3} - c\right)\mu^2 + \left(r^2 + \frac{80}{3} - \frac{8}{3}c\right)\mu + 20r^2 = 0. \tag{13}$$

According to Routh-Hurwitz criterion, if $c \in [-1.59, 7.75]$, then there exist a negative real eigenvalue and a pair of conjugate complex eigenvalues with positive real part.

For example, if $c = 2$, then the corresponding eigenvalues are $\mu_1 = 0$, $\mu_2 = -8$, $\mu_3 = -11.7318$, $\mu_4 = 0.5326 + 9.0302j$, and $\mu_5 = 0.5326 - 9.0302j$, which indicates that E_θ are unstable and saddle-foci with index two.

2.4 Bifurcation and chaos with different system parameter c

As it is well known, bifurcation diagram and Lyapunov exponent spectrum are two of the major methods for analyzing dynamical behaviors of a nonlinear system. Here, the classic fourth-order Runge-Kutta method is applied for the calculation of system (3). When the initial condition $\boldsymbol{u}_0 = (1, -1, 1, -1, 1)$, the bifurcation diagram and Lyapunov exponents of system (3) are shown in Fig. 1(a) and Fig. 1(b), respectively, where c varies at the range $[-2, 8]$ with the step size of $\Delta c = 0.01$. As shown in Fig. 1, system (3) is chaotic over most of the range $[-1.59, 7.75]$. Additionally, there exist some periodic windows at $c \in [4.50, 7.75]$, such as $W_1 = [4.592, 4.681]$, $W_2 = [4.703, 4.720]$, $W_3 = [5.762, 5.772]$, $W_4 = [5.828, 5.835]$, and $W_5 = [6.050, 6.062]$. Different periodic windows exhibit different periodic trajectories. In particular, we set $c = 2$ with the initial condition $\boldsymbol{u}_0 = (1, -1, 1, -1, 1)$, then all the five Lyapunov exponents of system (3) can be calculated as $\lambda_1 = 0.8580$, $\lambda_2 = 0$, $\lambda_3 = 0$, $\lambda_4 = -7.9995$, and $\lambda_5 = -11.5260$. Therefore, the Lyapunov dimension of system (3) is fractional, which is defined as

$$D_L = m + \frac{1}{|\lambda_{m+1}|}\sum_{k=1}^{m}\lambda_k = 3 + \frac{0.8580}{|-7.9995|} = 3.1073, \tag{14}$$

where m is the largest integer such that $\sum_{k=1}^{m}\lambda_k > 0$ and $\sum_{k=1}^{m+1}\lambda_k < 0$. Furthermore, the phase portrait on (u_1, u_5) plane and its corresponding Poincaré section generated in the hyperplane $u_5 = 18$ (which passes through the non-trivial equilibria) are plotted in Fig. 2(a) and Fig. 2(b), respectively. Obviously, as observed in Fig. 2, system (3) is chaotic in this case.

2.5 Coexistence of infinitely many attractors

Extreme multistability exhibits a rich diversity of stable states of a nonlinear dynamical system for a given set of parameters, and it indicates the great potential of such system in engineering applications. The coexistence of infinitely many attractors is found in system (3). For instance, phase portraits of five coexisting chaotic attractors ($c = 6.39$) as well as five coexisting periodic attractors ($c = 7.50$) of system (3) are shown in Fig. 3(a) and Fig. 3(b), respectively. As shown in Fig. 3, different colors represent different attractors with different initial conditions, where the blue attractors match $(1, 2, 3, 4, 5)$, the red attractors match $(2, 2, 3, 4, 5)$, the green attractors match $(3, 2, 3, 4, 5)$, the magenta attractors match $(4, 2, 3, 4, 5)$, and the cyan attractors match $(5, 2, 3, 4, 5)$. Moreover, it is well known that the basin of attraction is an effective method to detect the coexistence of attractors in a nonlinear system. In particular, when the initial condition of system (3) is given as $\boldsymbol{u}_0 = (u_1, u_2, 3, 4, 5)$, the basins of attraction with respect to different initial conditions at $c = 6.39$ and $c = 7.50$ are shown in Fig. 4(a) and Fig. 4(b), respectively, where $u_1 \in [-10, 10]$, $u_2 \in [-10, 10]$ and different colors represent different attractors. Obviously, due to the coexistence of infinitely many attractors, system (3) has the property of extreme multistability, and it reveals the complicated dynamical behaviors of the complex simplified Lorenz system.

3 The adaptive complex generalized function projective synchronization of the complex simplified Lorenz system with unknown parameter

In this section, based on Lyapunov stability theory, the adaptive complex generalized function projective synchronization between two complex simplified Lorenz systems with unknown parameter is investigated.

3.1 Mathematical model and problem description

Firstly, we consider the following n-dimensional complex drive system

$$\dot{\boldsymbol{x}} = \boldsymbol{F}(\boldsymbol{x})\boldsymbol{A} + \boldsymbol{f}(\boldsymbol{x}), \tag{15}$$

and the complex response system with adaptive controller is depicted as

$$\dot{\boldsymbol{y}} = \boldsymbol{G}(\boldsymbol{y})\boldsymbol{B} + \boldsymbol{g}(\boldsymbol{y}) + \boldsymbol{U}(\boldsymbol{x}, \boldsymbol{y}, \hat{\boldsymbol{A}}, \hat{\boldsymbol{B}}), \tag{16}$$

where $\boldsymbol{x} = (x_1, x_2, \cdots, x_n)^{\mathrm{T}} \in \mathbb{C}^n$ and $\boldsymbol{y} = (y_1, y_2, \cdots, y_n)^{\mathrm{T}} \in \mathbb{C}^n$ are complex state vectors of the complex drive system (15) and complex response system (16), respectively. $\boldsymbol{A} = (a_1, a_2, \cdots, a_p)^{\mathrm{T}} \in \mathbb{R}^p$ and $\boldsymbol{B} = (b_1, b_2, \cdots, b_q)^{\mathrm{T}} \in \mathbb{R}^q$ are real vectors of unknown parameters of the complex drive system (15) and complex response system (16), respectively. $\boldsymbol{F} : \mathbb{C}^{n\times 1} \to \mathbb{C}^{n\times p}$ is a $n \times p$ complex function matrix and $\boldsymbol{f} : \mathbb{C}^{n\times 1} \to \mathbb{C}^{n\times 1}$ is a $n \times 1$ complex function vector. $\boldsymbol{G} : \mathbb{C}^{n\times 1} \to \mathbb{C}^{n\times q}$ is a $n \times q$ complex function matrix and $\boldsymbol{g} : \mathbb{C}^{n\times 1} \to \mathbb{C}^{n\times 1}$

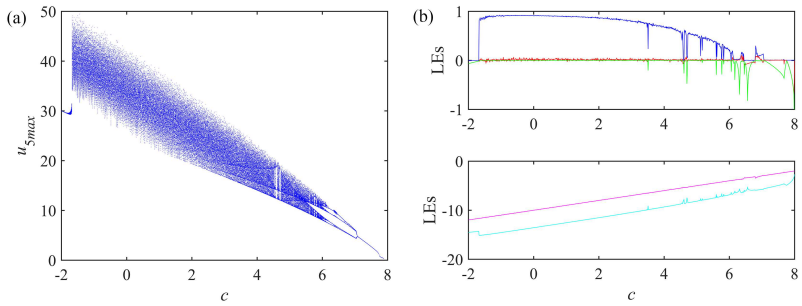

Fig. 1 Bifurcation diagram and Lyapunov exponents of system (3) for $c \in [-2, 8]$ with initial condition $\boldsymbol{u}_0 = (1, -1, 1, -1, 1)$ (**a**) Bifurcation diagram (**b**) Lyapunov exponents

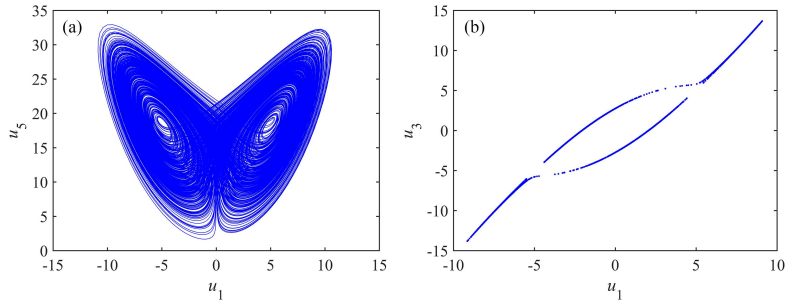

Fig. 2 Phase portrait and Poincaré section of system (3) for $c = 2$ with initial condition $\boldsymbol{u}_0 = (1, -1, 1, -1, 1)$ (**a**) Phase portrait (**b**) Poincaré section

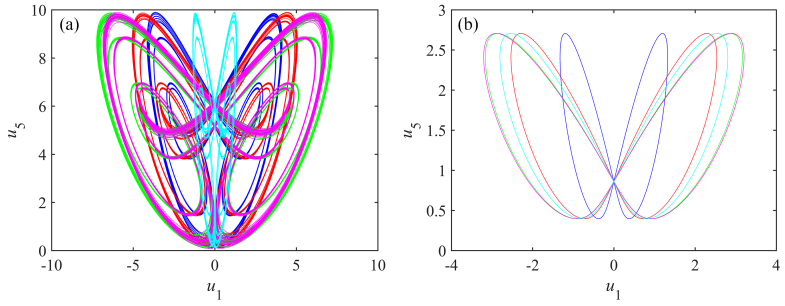

Fig. 3 Phase portraits of five coexisting chaotic attractors and five periodic attractors for (**a**) $c = 6.39$ (chaotic) and (**b**) $c = 7.50$ (periodic)

is a $n \times 1$ complex function vector. $\boldsymbol{U}(\boldsymbol{x}, \boldsymbol{y}, \hat{\boldsymbol{A}}, \hat{\boldsymbol{B}})$ is the undetermined adaptive controller. $\hat{\boldsymbol{A}}$, $\hat{\boldsymbol{B}}$ are parameter estimations of the unknown parameters $\boldsymbol{A}$ and $\boldsymbol{B}$. The adaptive complex generalized function projective synchronization error vector $\boldsymbol{e}(t)$ is defined as

$$\boldsymbol{e}(t) = \boldsymbol{y}(t) - \boldsymbol{\Phi}(t)\boldsymbol{x}(t), \tag{17}$$

where $\boldsymbol{\Phi}(t)$ is a non-diagonal complex function transformation matrix. Therefore, the adaptive complex generalized function projective synchronization error dynamical system is written as

$$\begin{aligned}\dot{\boldsymbol{e}}(t) =& \boldsymbol{G}(\boldsymbol{y})\boldsymbol{B} + \boldsymbol{g}(\boldsymbol{y}) - \boldsymbol{\Phi}(t)\boldsymbol{F}(\boldsymbol{x})\boldsymbol{A} - \boldsymbol{\Phi}(t)\boldsymbol{f}(\boldsymbol{x}) \\ & - \dot{\boldsymbol{\Phi}}(t)\boldsymbol{x} + \boldsymbol{U}(\boldsymbol{x}, \boldsymbol{y}, \hat{\boldsymbol{A}}, \hat{\boldsymbol{B}}).\end{aligned} \tag{18}$$

Next, we introduce the definition of adaptive complex generalized function projective synchronization of complex chaotic systems with unknown parameters.

Definition 1. For the complex drive system (15) and complex response system (16), if there exists an adaptive controller $\boldsymbol{U}(\boldsymbol{x}, \boldsymbol{y}, \hat{\boldsymbol{A}}, \hat{\boldsymbol{B}})$, such that $\lim_{t\to+\infty} \|\boldsymbol{y}(t) - \boldsymbol{\Phi}(t)\boldsymbol{x}(t)\| = \boldsymbol{0}$, then the adaptive complex generalized

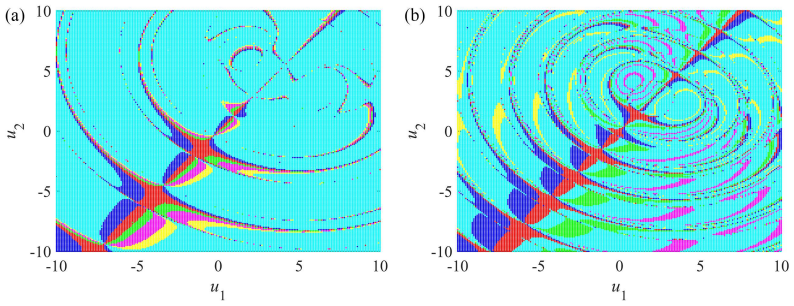

Fig. 4 Basins of attraction of system (3) for (**a**) $c = 6.39$ (chaotic) and (**b**) $c = 7.50$ (periodic) with initial condition $\boldsymbol{u}_0 = (u_1, u_2, 3, 4, 5)$

function projective synchronization between the complex drive system (15) and complex response system (16) is achieved asymptotically with respect to a non-diagonal complex function transformation matrix $\boldsymbol{\Phi}(t)$ when $t \to +\infty$, and the parameter estimations $\hat{\boldsymbol{A}}$, $\hat{\boldsymbol{B}}$ converge to the true values of the unknown parameters $\boldsymbol{A}$ and $\boldsymbol{B}$, respectively.

Theorem 1. For the given non-diagonal complex function transformation matrix $\boldsymbol{\Phi}(t)$, along with the initial conditions $\boldsymbol{x}(0)$ and $\boldsymbol{y}(0)$, if the adaptive controller $\boldsymbol{U}(\boldsymbol{x}, \boldsymbol{y}, \hat{\boldsymbol{A}}, \hat{\boldsymbol{B}})$ is designed as

$$\begin{aligned}\boldsymbol{U}(\boldsymbol{x}, \boldsymbol{y}, \hat{\boldsymbol{A}}, \hat{\boldsymbol{B}}) =& \boldsymbol{\Phi}(t)\boldsymbol{F}(\boldsymbol{x})\hat{\boldsymbol{A}} + \boldsymbol{\Phi}(t)\boldsymbol{f}(\boldsymbol{x}) + \dot{\boldsymbol{\Phi}}(t)\boldsymbol{x} \\ & - \boldsymbol{G}(\boldsymbol{y})\hat{\boldsymbol{B}} - \boldsymbol{g}(\boldsymbol{y}) + \boldsymbol{K}\boldsymbol{e},\end{aligned} \tag{19}$$

where $\boldsymbol{K} = \mathrm{diag}[k_1, k_2, \cdots, k_n]$ is a feedback gain matrix, whose diagonal elements are negative real constants, i.e., $k_l < 0\,(l = 1, 2, \cdots, n)$, and the corresponding parameter update laws are selected as

$$\begin{cases} \dot{\hat{\boldsymbol{A}}} = -\left(\boldsymbol{\Phi}^r(t)\boldsymbol{F}^r(\boldsymbol{x}) - \boldsymbol{\Phi}^i(t)\boldsymbol{F}^i(\boldsymbol{x})\right)^{\mathrm{T}} \boldsymbol{e}^r \\ \qquad\quad -\left(\boldsymbol{\Phi}^r(t)\boldsymbol{F}^i(\boldsymbol{x}) + \boldsymbol{\Phi}^i(t)\boldsymbol{F}^r(\boldsymbol{x})\right)^{\mathrm{T}} \boldsymbol{e}^i, \\ \dot{\hat{\boldsymbol{B}}} = \left(\boldsymbol{G}^r(\boldsymbol{y})\right)^{\mathrm{T}} \boldsymbol{e}^r + \left(\boldsymbol{G}^i(\boldsymbol{y})\right)^{\mathrm{T}} \boldsymbol{e}^i, \end{cases} \tag{20}$$

then the adaptive complex generalized function projective synchronization between the complex drive system (15) and complex response system (16) is achieved asymptotically when $t \to +\infty$, and $\hat{\boldsymbol{A}}, \hat{\boldsymbol{B}}$ converge to the true values of $\boldsymbol{A}$ and $\boldsymbol{B}$, respectively.

Hypothesis For the given non-diagonal complex function transformation matrix $\boldsymbol{\Phi}(t)$, along with the complex function matrices $\boldsymbol{F}(\boldsymbol{x})$ and $\boldsymbol{G}(\boldsymbol{y})$, the complex function vector group, consisting of all the columns of $\boldsymbol{\Phi}(t)\boldsymbol{F}(\boldsymbol{x})$ and $-\boldsymbol{G}(\boldsymbol{y})$, is linear independence.

Proof Substituting Eq. (19) into Eq. (18), we have

$$\dot{\boldsymbol{e}}(t) = \boldsymbol{\Phi}(t)\boldsymbol{F}(\boldsymbol{x})\tilde{\boldsymbol{A}} - \boldsymbol{G}(\boldsymbol{y})\tilde{\boldsymbol{B}} + \boldsymbol{K}\boldsymbol{e}, \tag{21}$$

where $\tilde{\boldsymbol{A}} = \hat{\boldsymbol{A}} - \boldsymbol{A}$ and $\tilde{\boldsymbol{B}} = \hat{\boldsymbol{B}} - \boldsymbol{B}$ are estimation errors of the unknown parameters $\boldsymbol{A}$ and $\boldsymbol{B}$, respectively.

The Lyapunov function candidate is chosen as

$$\begin{aligned}V\left(\boldsymbol{e}^r, \boldsymbol{e}^i, \tilde{\boldsymbol{A}}, \tilde{\boldsymbol{B}}\right) = \frac{1}{2}\Big(&\left(\boldsymbol{e}^r\right)^{\mathrm{T}} \boldsymbol{e}^r + \left(\boldsymbol{e}^i\right)^{\mathrm{T}} \boldsymbol{e}^i \\ &+ \tilde{\boldsymbol{A}}^{\mathrm{T}}\tilde{\boldsymbol{A}} + \tilde{\boldsymbol{B}}^{\mathrm{T}}\tilde{\boldsymbol{B}}\Big),\end{aligned} \tag{22}$$

and its derivative with respect to time is

$$\dot{V}\left(\boldsymbol{e}^r, \boldsymbol{e}^i, \tilde{\boldsymbol{A}}, \tilde{\boldsymbol{B}}\right) = \left(\boldsymbol{e}^r\right)^{\mathrm{T}} \boldsymbol{K}\boldsymbol{e}^r + \left(\boldsymbol{e}^i\right)^{\mathrm{T}} \boldsymbol{K}\boldsymbol{e}^i. \tag{23}$$

Obviously, $\dot{V}$ is negative semi-definite, thus we can't conclude directly that system (21) is stable asymptotically at the origin. However, according to Eq. (22) and Eq. (23), we know that $V(t)$ is bounded owing to $0 \le V(t) \le V(0)$, and we can also conclude that $\boldsymbol{e}^r$, $\boldsymbol{e}^i$, $\tilde{\boldsymbol{A}}$, $\tilde{\boldsymbol{B}}$ are bounded. Therefore, $\dot{\boldsymbol{e}}$ exists and is finite. In addition, from Eq. (23), we know that $\dot{V} \le k_{max}|\boldsymbol{e}|^2$, i.e., $|\boldsymbol{e}|^2 \le \dot{V}/k_{max}$, where $k_{max} = \max(k_1, k_2, \cdots, k_n)$. Hence, we have $\int_0^t |\boldsymbol{e}(\tau)|^2 \mathrm{d}\tau \le (V(t) - V(0))/k_{max} \le -V(0)/k_{max}$, which means that $\boldsymbol{e}(t)$ is square integrable. According to the Barbalat's lemma [38], we can finally draw the conclusion that $\lim_{t\to+\infty} \boldsymbol{e}(t) = \boldsymbol{0}$. Consequently, the adaptive complex generalized function projective synchronization between the complex drive system (15) and complex response system (16) is achieved asymptotically with respect to a non-diagonal complex function transformation matrix $\boldsymbol{\Phi}(t)$ by using the adaptive controller (19) and parameter adaptive laws (20). Besides, according to the LaSalle's invariance principle [39], the maximal invariant set can be written as

$$\begin{aligned}\boldsymbol{M} = \Big\{\boldsymbol{e}, \tilde{\boldsymbol{A}}, \tilde{\boldsymbol{B}} \,\Big|\, &\boldsymbol{e} = \boldsymbol{0}, \dot{\boldsymbol{e}}(t) = \boldsymbol{\Phi}(t)\boldsymbol{F}(\boldsymbol{x})\tilde{\boldsymbol{A}} - \boldsymbol{G}(\boldsymbol{y})\tilde{\boldsymbol{B}} \\ &+ \boldsymbol{K}\boldsymbol{e} = \boldsymbol{0}\Big\}.\end{aligned} \tag{24}$$

Therefore, we have $\boldsymbol{\Phi}(t)\boldsymbol{F}(\boldsymbol{x})\tilde{\boldsymbol{A}} - \boldsymbol{G}(\boldsymbol{y})\tilde{\boldsymbol{B}} = \boldsymbol{0}$, and due to the linear independence hypothesis, we can conclude that $\tilde{\boldsymbol{A}} = \boldsymbol{0}$ and $\tilde{\boldsymbol{B}} = \boldsymbol{0}$, i.e., the unknown parameters $\boldsymbol{A}$ and $\boldsymbol{B}$ can be correctly identified. The proof is completed.

Corollary 1. If the structures of the complex drive system (15) and complex response system (16) are identical, i.e., $\boldsymbol{F}(\cdot)=\boldsymbol{G}(\cdot)$, $\boldsymbol{f}(\cdot)=\boldsymbol{g}(\cdot)$, and $\boldsymbol{A}=\boldsymbol{B}$, then the adaptive controller $\boldsymbol{U}(\boldsymbol{x},\boldsymbol{y},\hat{\boldsymbol{A}})$ is designed as

$$\begin{aligned}\boldsymbol{U}(\boldsymbol{x},\boldsymbol{y},\hat{\boldsymbol{A}})=&(\boldsymbol{\Phi}(t)\boldsymbol{F}(\boldsymbol{x})-\boldsymbol{F}(\boldsymbol{y}))\hat{\boldsymbol{A}}+\boldsymbol{\Phi}(t)\boldsymbol{f}(\boldsymbol{x})\\&+\dot{\boldsymbol{\Phi}}(t)\boldsymbol{x}-\boldsymbol{f}(\boldsymbol{y})+\boldsymbol{K}\boldsymbol{e},\end{aligned}\tag{25}$$

where $\boldsymbol{K}=\mathrm{diag}[k_1,k_2,\cdots,k_n]$ is a feedback gain matrix, whose diagonal elements are negative real constants, i.e., $k_l<0\,(l=1,2,\cdots,n)$, and the corresponding parameter update laws are selected as

$$\begin{aligned}\dot{\hat{\boldsymbol{A}}}=&\left(\boldsymbol{F}^r(\boldsymbol{y})-\boldsymbol{\Phi}^r(t)\boldsymbol{F}^r(\boldsymbol{x})+\boldsymbol{\Phi}^i(t)\boldsymbol{F}^i(\boldsymbol{x})\right)^{\mathrm{T}}\boldsymbol{e}^r\\&+\left(\boldsymbol{F}^i(\boldsymbol{y})-\boldsymbol{\Phi}^r(t)\boldsymbol{F}^r(\boldsymbol{x})-\boldsymbol{\Phi}^i(t)\boldsymbol{F}^i(\boldsymbol{x})\right)^{\mathrm{T}}\boldsymbol{e}^i.\end{aligned}\tag{26}$$

Hence, the adaptive complex generalized function projective synchronization between two identical complex chaotic systems with unknown parameters is achieved asymptotically when $t\to+\infty$, and $\hat{\boldsymbol{A}}$ converges to the true values of $\boldsymbol{A}$.

3.2 Numerical simulations and discussion

To observe the adaptive complex generalized function projective synchronization between two complex simplified Lorenz systems with unknown parameter, we define the complex drive system as

$$\begin{cases}\dot{x}_1=10(x_2-x_1),\\ \dot{x}_2=(24-4c)x_1+cx_2-x_1x_3,\\ \dot{x}_3=-8x_3/3+1/2(\bar{x}_1x_2+x_1\bar{x}_2),\end{cases}\tag{27}$$

and the complex response system with adaptive controllers is depicted as

$$\begin{cases}\dot{y}_1=10(y_2-y_1)+v_1,\\ \dot{y}_2=(24-4c)y_1+cy_2-y_1y_3+v_2,\\ \dot{y}_3=-8y_3/3+1/2(\bar{y}_1y_2+y_1\bar{y}_2)+v_3,\end{cases}\tag{28}$$

where v_1,v_2,v_3 are undetermined adaptive controllers, and c is the unknown parameter. If the non-diagonal complex function transformation matrix $\boldsymbol{\Phi}(t)$ is chosen as

$$\boldsymbol{\Phi}(t)=\begin{pmatrix}0&e^{jt}&0\\ e^{2jt}&0&0\\ 0&0&\cos 3t\end{pmatrix},\tag{29}$$

then the errors between the complex drive system (27) and complex response system (28) are expressed by

$$\begin{cases}e_1=y_1-e^{jt}x_2,\\ e_2=y_2-e^{2jt}x_1,\\ e_3=y_3-x_3\cos 3t,\end{cases}\tag{30}$$

therefore, the adaptive complex generalized function projective synchronization error dynamical system is written as

$$\begin{cases}\dot{e}_1=&10(y_2-y_1)-e^{jt}\left[(24-4c)x_1+cx_2-x_1x_3\right]\\&-je^{jt}x_2+v_1,\\ \dot{e}_2=&(24-4c)y_1+cy_2-y_1y_3-10e^{2jt}(x_2-x_1)\\&-2je^{2jt}x_1+v_2,\\ \dot{e}_3=&-8y_3/3+1/2(\bar{y}_1y_2+y_1\bar{y}_2)+\cos 3t\,[8x_3/3\\&-1/2(\bar{x}_1x_2+x_1\bar{x}_2)]+3x_3\sin 3t+v_3.\end{cases}\tag{31}$$

According to Theorem 1, if the adaptive controllers v_1,v_2,v_3 are designed as

$$\begin{cases}v_1=&10(y_1-y_2)+e^{jt}[(24-4\hat{c})x_1+\hat{c}x_2-x_1x_3]\\&+je^{jt}x_2+k_1e_1,\\ v_2=&(4\hat{c}-24)y_1-\hat{c}y_2+y_1y_3+10e^{2jt}(x_2-x_1)\\&+2je^{2jt}x_1+k_2e_2,\\ v_3=&8y_3/3-1/2(\bar{y}_1y_2+y_1\bar{y}_2)-\cos 3t\,[8x_3/3\\&-1/2(\bar{x}_1x_2+x_1\bar{x}_2)]-3x_3\sin 3t+k_3e_3,\end{cases}\tag{32}$$

where $\hat{c}$ is the estimation of the unknown parameter c, and its parameter update law is selected as

$$\begin{aligned}\dot{\hat{c}}=&e_1^r\left(4x_1^r\cos t+x_2^i\sin t-4x_1^i\sin t-x_2^r\cos t\right)\\&+e_1^i\left(4x_1^r\sin t+4x_1^i\cos t-x_2^r\sin t-x_2^i\cos t\right)\\&+e_2^r\left(y_2^r-4y_1^r\right)+e_2^i\left(y_2^i-4y_1^i\right),\end{aligned}\tag{33}$$

then the adaptive complex generalized function projective synchronization between the complex drive system (27) and response system (28) with unknown parameter c is achieved asymptotically when $t\to+\infty$, and $\hat{c}$ converges to the true value of c.

In the numerical simulations, let $c=2$. In this case, the complex simplified Lorenz system behaves chaotically. The initial conditions are randomly selected as $\boldsymbol{x}(0)=(1+2j,3+4j,5)$ and $\boldsymbol{y}(0)=(6+7j,8+9j,10)$. The initial value of the parameter estimation $\hat{c}$ and the feedback gain matrix $\boldsymbol{K}$ are set as $\hat{c}(0)=2.5$ and $\boldsymbol{K}=\mathrm{diag}[-5,-5,-5]$, respectively. Time evolutions of the synchronization error and parameter estimation are plotted in Fig. 5, where $|e|=\sqrt{|e_1|^2+|e_2|^2+|e_3|^2}$. As observed in Fig. 5, the numerical simulation results illustrate that the adaptive complex generalized function projective synchronization between the complex drive system (27) and complex response system (28) has been achieved almost within two seconds, and the unknown parameter c is successfully identified. Additionally, the feedback gain matrix $\boldsymbol{K}$ has a great effect on the performance of the proposed synchronization scheme. Time

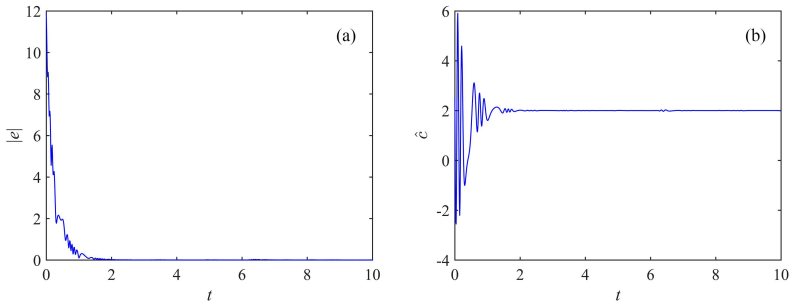

Fig. 5 Time evolutions of the synchronization error and parameter estimation (**a**) $|e|$ versus t (**b**) $\hat{c}$ versus t

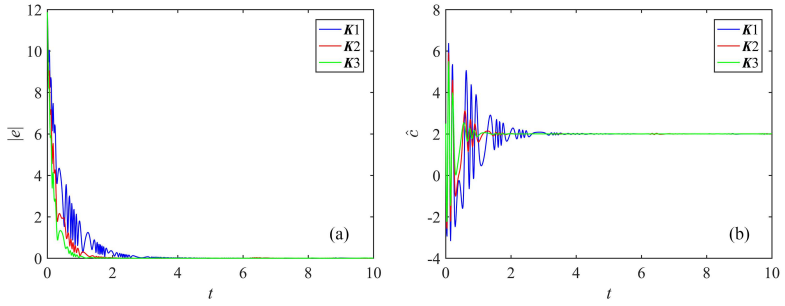

Fig. 6 Time evolutions of the synchronization error and parameter estimation with different feedback gain matrices (**a**) $|e|$ versus t (**b**) $\hat{c}$ versus t

evolutions of the synchronization error and parameter estimation with different feedback gain matrices are plotted in Fig. 6, where $\boldsymbol{K}1 = \mathrm{diag}[-3,-3,-3]$, $\boldsymbol{K}2 = \mathrm{diag}[-5,-5,-5]$, and $\boldsymbol{K}3 = \mathrm{diag}[-7,-7,-7]$. Obviously, as shown in Fig. 6, the adaptive complex generalized function projective synchronization between the complex drive system (27) and complex response system (28) is achieved more rapidly with a stronger feedback gain matrix. Meanwhile, the unknown parameter c is also identified more quickly.

4 Conclusions

In this paper, by extending the real state variables from real domain to complex domain, the complex simplified Lorenz system is proposed. Dynamics and synchronization of the proposed system are investigated theoretically and numerically. The results show that the complex simplified Lorenz system has non-trivial circular equilibria and displays abundant and complicated dynamical behaviors. Particularly, the coexistence of infinitely many attractors, i.e., extreme multistability, is revealed by phase portraits and basins of attraction. Furthermore, the adaptive complex generalized function projective synchronization between two complex simplified Lorenz systems with unknown parameter is achieved. Based on Lyapunov stability theory, the corresponding adaptive controllers and parameter update law are designed. The numerical simulation results demonstrate the effectiveness and feasibility of the proposed synchronization scheme. Additionally, it is found that the feedback gain matrix has a great effect on the performance of the proposed synchronization scheme. With a stronger feedback gain matrix, the synchronization between the complex drive system and complex response system is achieved more rapidly, and the unknown parameter is also identified more quickly. The proposed synchronization scheme can be applied to secure communication for higher transmission efficiency and security performance due to the complex variables, unknown parameters, and unpredictable non-diagonal complex function transformation matrix. Next, we will try to study the hardware implementation and engineering applications of the complex simplified Lorenz system.

Acknowledgements This work was supported by the National Natural Science Foundation of China (Grant Nos. 62071496, 62061008, and 61901530).

Conflict of interest

The authors declare that they have no conflict of interest.

References

1. Lorenz, E.N.: Deterministic nonperiodic flow. J. Atmos. Sci. **20**(2), 130–141 (1963)
2. Fowler, A.C., Gibbon, J.D., McGuinness, M.J.: The complex Lorenz equations. Physica D **4**(2), 139–163 (1982)
3. Gibbon, J.D., McGuinness, M.J.: The real and complex Lorenz equations in rotating fluids and lasers. Physica D **5**(1), 108–122 (1982)
4. Fowler, A.C., Gibbon, J.D., McGuinness, M.J.: The real and complex Lorenz equations and their relevance to physical systems. Physica D **7**(1-3), 126–134 (1983)
5. Ning, C.Z., Haken, H.: Detuned lasers and the complex Lorenz equations: subcritical and supercritical hopf bifurcations. Phys. Rev. A **41**(7), 3826–3837 (1990)
6. Mahmoud, G.M., Mohamed, A.A., Aly, S.A.: Strange attractors and chaos control in periodically forced complex Duffing's oscillators. Physica A **292**(1-4), 193–206 (2001)
7. Mahmoud, G.M., Bountis, T.: The dynamics of systems of complex nonlinear oscillators: a review. Int. J. Bifurcat. Chaos **14**(11), 3821–3846 (2004)
8. Mahmoud, G.M., Mahmoud, E.E., Arafa, A.A.: On projective synchronization of hyperchaotic complex nonlinear systems based on passive theory for secure communications. Phys. Scr. **87**(5), 055002 (2013)
9. Liu, S.T., Zhang, F.F.: Complex function projective synchronization of complex chaotic system and its applications in secure communication. Nonlinear Dyn. **76**(2), 1087–1097 (2014)
10. Wu, X.J., Zhu, C.J., Kan, H.B.: An improved secure communication scheme based passive synchronization of hyperchaotic complex nonlinear system. Appl. Math. Comput. **252**, 201–214 (2015)
11. Wang, L.Y., Song, H.J., Liu, P.: A novel hybrid color image encryption algorithm using two complex chaotic systems. Opt. Lasers Eng. **77**, 118–125 (2016)
12. Liu, H.J., Zhang, Y.Q., Kadir, A., Xu, Y.Q.: Image encryption using complex hyper chaotic system by injecting impulse into parameters. Appl. Math. Comput. **360**, 83–93 (2019)
13. Mahmoud, G.M., Bountis, T., Mahmoud, E.E.: Active control and global synchronization of the complex Chen and Lü systems. Int. J. Bifurcat. Chaos **17**(12), 4295–4308 (2007)
14. Mahmoud, G.M., Ahmed, M.E., Mahmoud, E.E.: Analysis of hyperchaotic complex Lorenz systems. Int. J. Mod. Phys. C **19**(10), 1477–1494 (2008)
15. Mahmoud, G.M., Mahmoud, E.E., Ahmed, M.E.: On the hyperchaotic complex Lü system. Nonlinear Dyn. **58**(4), 725–738 (2009)
16. Mahmoud, G.M., Mahmoud, E.E.: Complete synchronization of chaotic complex nonlinear systems with uncertain parameters. Nonlinear Dyn. **62**(4), 875–882 (2010)
17. Mahmoud, G.M., Mahmoud, E.E.: Lag synchronization of hyperchaotic complex nonlinear systems. Nonlinear Dyn. **67**(2), 1613–1622 (2012)
18. Mahmoud, G.M., Mahmoud, E.E.: Complex modified projective synchronization of two chaotic complex nonlinear systems. Nonlinear Dyn. **73**(4), 2231–2240 (2013)
19. Liu, D.F., Wu, Z.Y., Ye, Q.L.: Adaptive impulsive synchronization of uncertain drive-response complex-variable chaotic systems. Nonlinear Dyn. **75**(1), 209–216 (2014)
20. Liu, J., Liu, S.T., Yuan, C.H.: Adaptive complex modified projective synchronization of complex chaotic (hyperchaotic) systems with uncertain complex parameters. Nonlinear Dyn. **79**(2), 1035–1047 (2015)
21. Sun, J.W., Cui, G.Z., Wang, Y.F., Shen, Y.: Combination complex synchronization of three chaotic complex systems. Nonlinear Dyn. **79**(2), 953–965 (2015)
22. Liu, J., Liu, S.T., Sprott, J.C.: Adaptive complex modified hybrid function projective synchronization of different dimensional complex chaos with uncertain complex parameters. Nonlinear Dyn. **83**(1-2), 1109–1121 (2016)
23. Liu, J., Liu, S.T.: Complex modified function projective synchronization of complex chaotic systems with known and unknown complex parameters. Appl. Math. Model. **48**, 440–450 (2017)
24. Wang, S.B., Wang, X.Y., Zhou, Y.F., Han, B.: A memristor-based hyperchaotic complex Lü system and its adaptive complex generalized synchronization. Entropy **18**(2), 58 (2016)
25. Yu, Y.G., Li, H.X.: Adaptive generalized function projective synchronization of uncertain chaotic systems. Nonlinear Anal. Real World Appl. **11**(4), 2456–2464 (2010)
26. Wu, X.J., Wang, H., Lu, H.T.: Hyperchaotic secure communication via generalized function projective synchronization. Nonlinear Anal. Real World Appl. **12**(2), 1288–1299 (2011)
27. Hens, C., Dana, S.K., Feudel, U.: Extreme multistability: attractor manipulation and robustness. Chaos **25**(5), 053112 (2015)
28. Yuan, F., Wang, G.Y., Wang, X.W.: Extreme multistability in a memristor-based multi-scroll hyper-chaotic system. Chaos **26**(7), 073107 (2016)
29. Bao, B.C., Xu, Q., Bao, H., Chen, M.: Extreme multistability in a memristive circuit. Electron. Lett. **52**(12), 1008–1010 (2016)
30. Bao, B.C., Jiang, T., Xu, Q., Chen, M., Wu, H.G., Hu, Y.H.: Coexisting infinitely many attractors in active bandpass filter-based memristive circuit. Nonlinear Dyn. **86**(3), 1711–1723 (2016)
31. Bao, B.C., Jiang, T., Wang, G.Y., Jin, P.P., Bao, H., Chen, M.: Two-memristor-based Chua's hyperchaotic circuit with plane equilibrium and its extreme multistability. Nonlinear Dyn. **89**(2), 1157–1171 (2017)
32. Bao, B.C., Bao, H., Wang, N., Chen, M., Xu, Q.: Hidden extreme multistability in memristive hyperchaotic system. Chaos Solitons Fractals **94**, 102–111 (2017)
33. Lai, Q., Kuate, P.D.K., Liu, F., Iu, H.H.C.: An extremely simple chaotic system with infinitely many coexisting attractors. IEEE Trans. on Circuits Syst. II Express Briefs **67**(6), 1129–1133 (2019)
34. Sprott, J.C.: Some simple chaotic flows. Phys. Rev. E **50**(2), 647–650 (1994)
35. Li, C.B., Lu, T.N., Chen, G.R., Xing, H.Y.: Doubling the coexisting attractors. Chaos **29**(5), 051102 (2019)
36. Lai, Q., Chen, S.M.: Generating multiple chaotic attractors from Sprott B system. Int. J. Bifurcat. Chaos **26**(11), 1650177 (2016)
37. Sun, K.H., Sprott, J.C.: Dynamics of a simplified Lorenz system. Int. J. Bifurcat. Chaos **19**(4), 1357–1366 (2009)
38. Tao, G.: A simple alternative to the Barbalat lemma. IEEE Trans. Automat. Contr. **42**(5), 698 (1997)
39. Khalil, H.K., Grizzle, J.W.: Nonlinear systems, third edition. Prentice Hall, Englewood Cliffs (2002)

Figures

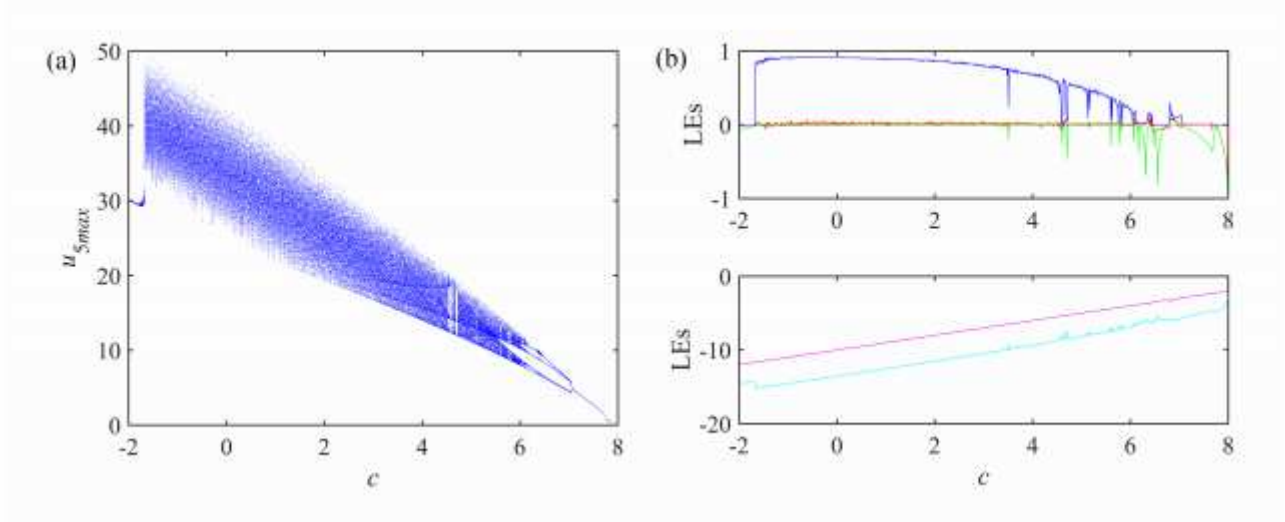

Figure 1

Bifurcation diagram and Lyapunov exponents of system (3) for c ∈ [−2, 8] with initial condition u0 = (1, −1, 1, −1, 1) (a) Bifurcation diagram (b) Lyapunov exponents

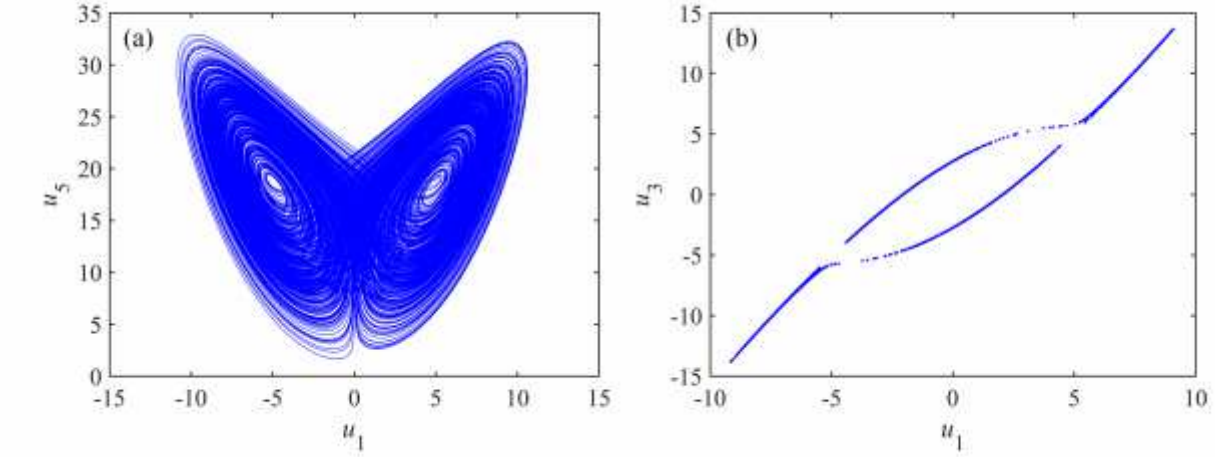

Figure 2

Phase portrait and Poincaré section of system (3) for c = 2 with initial condition u0 = (1, −1, 1, −1, 1) (a) Phase portrait (b) Poincaré section

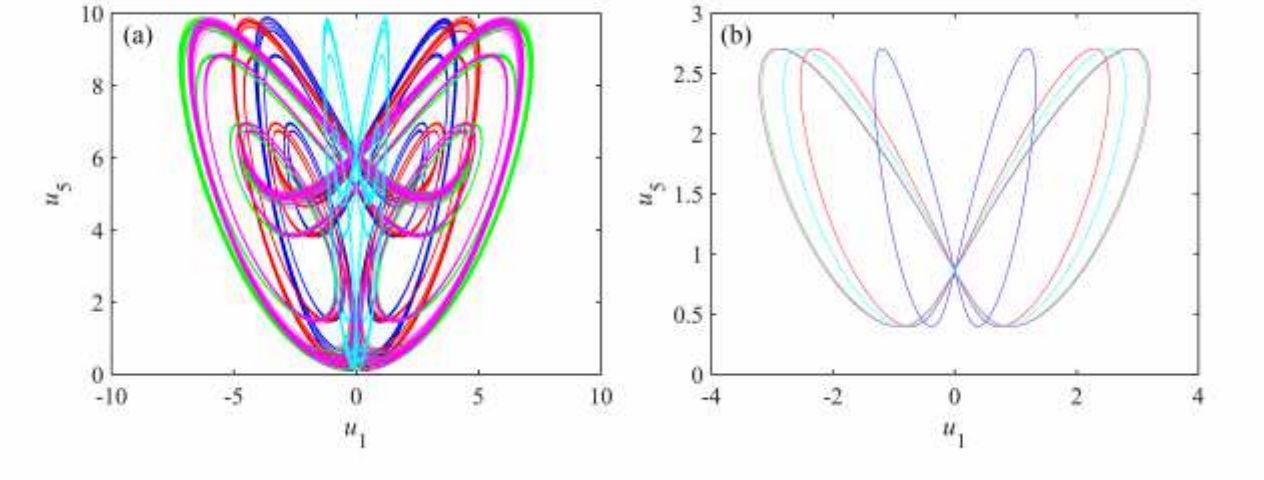

Figure 3

Phase portraits of five coexisting chaotic attractors and five periodic attractors for (a) c = 6.39 (chaotic) and (b) c = 7.50 (periodic)

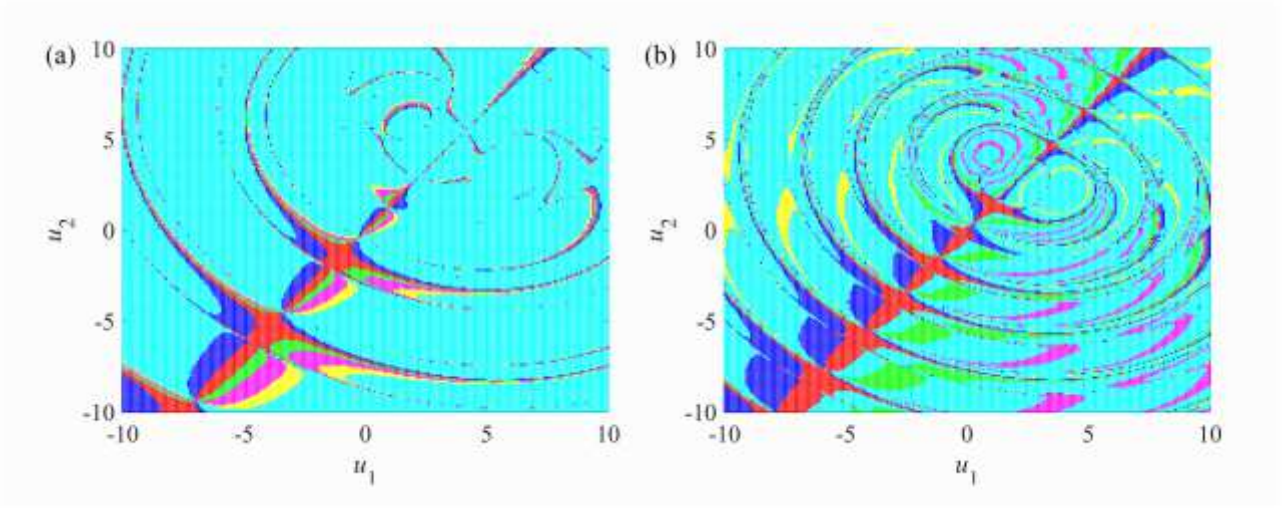

Figure 4

Basins of attraction of system (3) for (a) c = 6.39 (chaotic) and (b) c = 7.50 (periodic) with initial condition u0 = (u1, u2, 3, 4, 5)

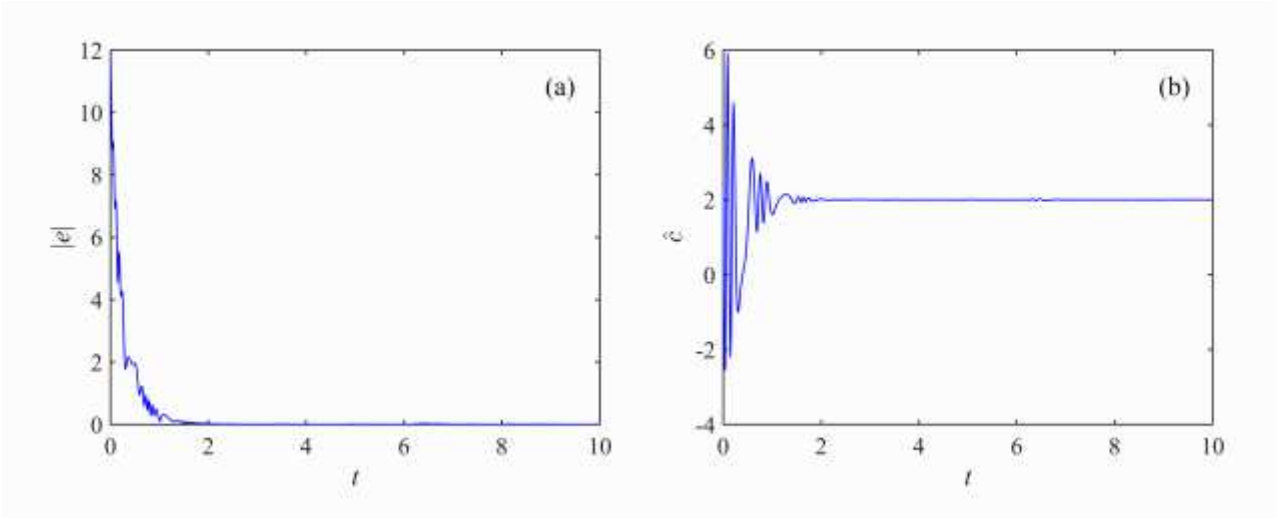

Figure 5

Time evolutions of the synchronization error and parameter estimation (a) |e| versus t (b) cˆ versus t

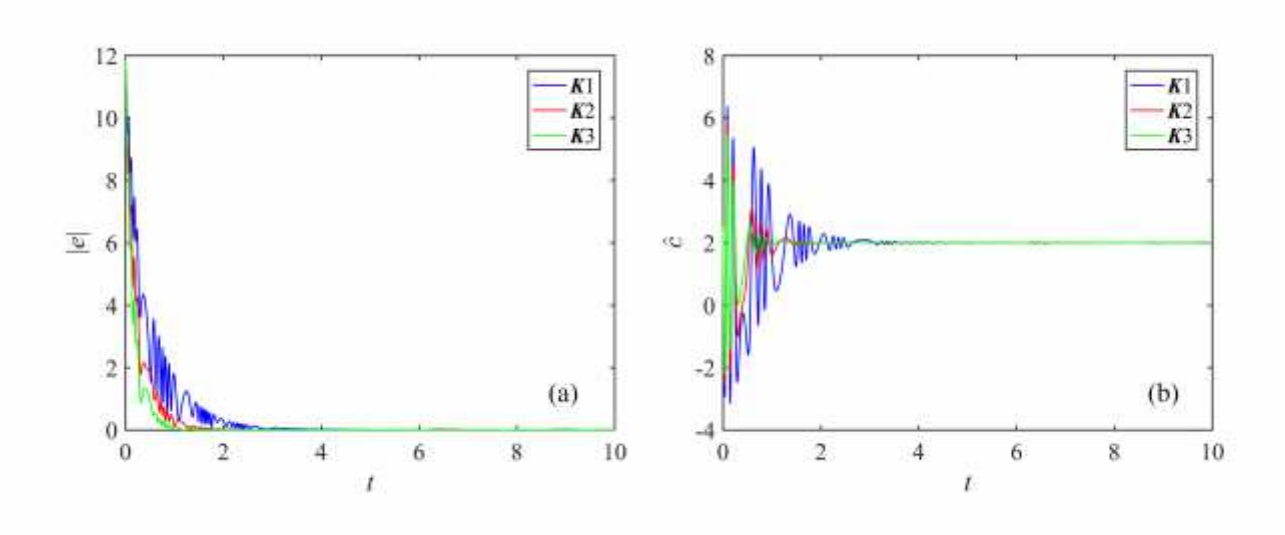

Figure 6

Time evolutions of the synchronization error and parameter estimation with different feedback gain matrices (a) |e| versus t (b) cˆ versus t